Segmental Dynamics of Bulk Polymers Studied by Fluorescence Correlation Spectroscopy

Andreas Best,[†] Tadeusz Pakula,[†] and George Fytas*,[†,‡]

Max Planck Institute for Polymer Research, P.O. Box 3148, 55021 Mainz, Germany, and F.O.R.T.H. and Department of Materials Science and Technology, University of Crete, P.O. Box 1527, 71110 Heraklion, Greece

Received December 14, 2004
Revised Manuscript Received February 7, 2005

Fluorescence correlation spectroscopy (FCS) has been successfully utilized to study transport properties in various biological environments[1,2] while applications in other soft systems are rare.[3,4] In FCS, the concept is that the fluorescent molecules diffusing in to and out of the laser focus cause detectable fluctuations of fluorescence intensity which can be directly correlated with the fluctuation of the number of the fluorescent species in the small volume. Hence, the translational diffusion of extremely dilute tagged molecules controls the decay of the intensity autocorrelation function $C(t)$. Diffusion of small probes in polymers influences several processes such as plasticization, drug delivery, coloration, permeation reaction kinetics, etc. The correlation function $C(t)$ yields information about dynamics of the fluorescing probes and about the medium in which they are dispersed or anchored. An access to the dynamics of the medium depends, however, on the strength of dynamic coupling of the small probes with the conformational rearrangements in the polymer matrix. Probe diffusion in dense polymer systems can be measured by grating techniques such as fluorescence recovery after bleaching (FRAP)[5] and forced Rayleigh light scattering (FRS) methods,[6,7] but we are not aware of any similar application[4,8] to local polymer dynamics by FCS.

In this short report, we show that FCS can probe segmental dynamics of amorphous bulk polymers at temperatures above the glass transition. The translational diffusion coefficient D_s of the fluorescent molecular tracer correlates with the segmental relaxation time of the polymer matrix, assuming a reasonable value for the cooperative length relevant for its glass transition. The same is demonstrated for a molecular glass former with considerably faster local mobility. It is, therefore, the local dynamics and not the macroscopic shear viscosity (related to chain dynamics) that controls D_s in the case of polymer melts.

Three samples of amorphous poly(*n*-butyl acrylate) (PBA) with weight-average molar mass M_w, polydispersity M_w/M_n, and glass transition temperature T_g listed in Table 1 were employed in the present study.[9] To substantially vary the local dynamics, we deliberately included in this investigation dibutyl phthalate (DBP), an often used plasticizer with low T_g (Table 1). The segmental relaxation time τ_s was obtained[10] both from the dielectric loss $M''(\omega)$ measured by dielectric spectroscopy (DS) due to the dipole moment of the polymer repeat unit and from the viscoelastic spectra determined using mechanical spectroscopy (MS). Figure 1a shows the dielectric modulus $M^*(\omega) = 1/\epsilon^*(\omega)$ (real $M'(\omega)$ and imaginary $M''(\omega)$ parts) at different temperatures superimposed by the horizontal shift (a_T) relative to the spectrum at $T_{ref} = 254$ K. At T_{ref}, $\tau_s \cong 15$ μs (vertical dashed line) while the lack of successful $t-T$ (time−temperature) superposition at high frequencies is expected due to the presence of a secondary β-relaxation, a thermally activated process.[11]

Table 1. Properties of the Poly(*n*-butyl acrylate) (P1−P3) and Dibutyl Phthalate (DBP) Samples

sample	M_w (kg/mol)	M_w/M_n	T_g [K]	τ_c (ms)[a,b]	τ_s (ns)[a,b]	τ_D (ms)[a]
P1	13.3	1.20	223.5	0.17	22	65
P2	36	1.13	224.7	1.6	26	60
P3	61.3	1.09	226.0	21.2	28	60
DBP	0.278		181.0		0.25	1.2

[a] The relaxation times correspond to $T_{ref} = 295$ K. [b] Estimated error ∼10%.

Complementarily, MS measures the shear modulus $G^*(\omega)$ at different temperatures. The $t-T$ superimposed real (G') and imaginary (G'') parts at $T_{ref} = 254$ K are shown in Figure 1b. Both the segmental relaxation time τ_s and the chain relaxation time τ_c are readily identified in Figure 1b by the corresponding relaxation frequencies (dashed vertical lines). The segmental τ_s from DS and MS assume comparable values. The value of τ_s is virtually independent of the PBA chain length and at 295 K ($= T_g + 70$ K) amounts to 25 ± 3 ns (Table 1). On the contrary, the overall chain relaxation time τ_c obtained from MS exhibits the expected strong ($\sim M_w^{3.3}$) molecular weight dependence as shown by the values of τ_c at 295 K in Table 1.

The primary α-relaxation time τ_s (=0.25 ns) in DBP at 295 K is much shorter than the segmental time in PBA as expected from the lower T_g value in DBP (Table 1). This large change in τ_s can be hardly achieved by temperature variation; for all fragile glasses $\tau_s(T)$ levels off in the nanosecond range and hence at temperatures far above T_g. FCS is therefore challenged to capture this vastly different τ_s (by almost 2 orders of magnitude) in DBP and PBA.

Films of PBA doped by rhodamine Rh6G at a concentration of about 0.5 μM were prepared by casting from a mixture of solutions of Rh6G in water and PBA in THF and subsequent removal of the solvents by heating at 65 °C at 1 mbar. The same procedure was followed for the introduction of the Rh6G into DBP. The fluorescence intensity autocorrelation function, $C(t)$, in the films of an average thickness ∼100 μm was recorded with a confocal system using the Axiovert 200M microscope Confocor 2 and the C-Apochromat 40×/1.2 W objective (Carl Zeiss, Jena, Germany). For the excitation, the 488 nm line of a 25 mW argon laser was used. The fluorescence was recorded for wavelengths in the range 530−600 nm by single photon counting using an avalanche photodiode. The focus dimensions (diameter $2r_0 = 320$ nm and height $2z_0 = 1650$ nm) were determined for the Rh6G water solution, and the difference in the refractive index with respect to the polymer was considered using a suitable objective. $C(t)$ was obtained by the sum of 20 runs of 60 s duration each. Figure 2 shows the experimental $C(t)$ for the Rh6G in PBA(P1)

[†] Max Planck Institute for Polymer Research.
[‡] University of Crete.

10.1021/ma047430k CCC: $30.25
Published on Web 04/14/2005

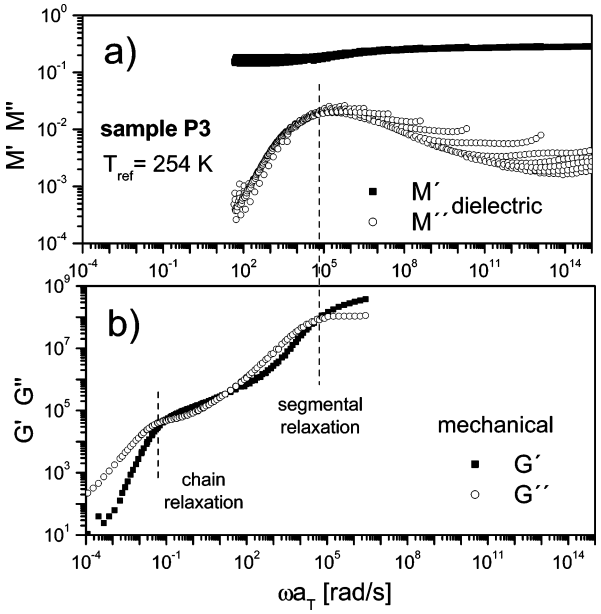

Figure 1. Superimposed dielectric modulus components ($M'(\omega)$ and $M''(\omega)$) (temperature range 175−300 K) (a) and dynamic shear modulus ($G'(\omega)$ and $G''(\omega)$) (b) obtained at different temperatures (from T_g up to T_g + 60 K) for the amorphous poly(butyl acrylate) (P3 sample) vs the reduced frequency (ωa_T). The dashed lines indicate the relaxation frequencies $1/\tau_s$ and $1/\tau_c$ at the reference temperature T_{ref} = 254 K.

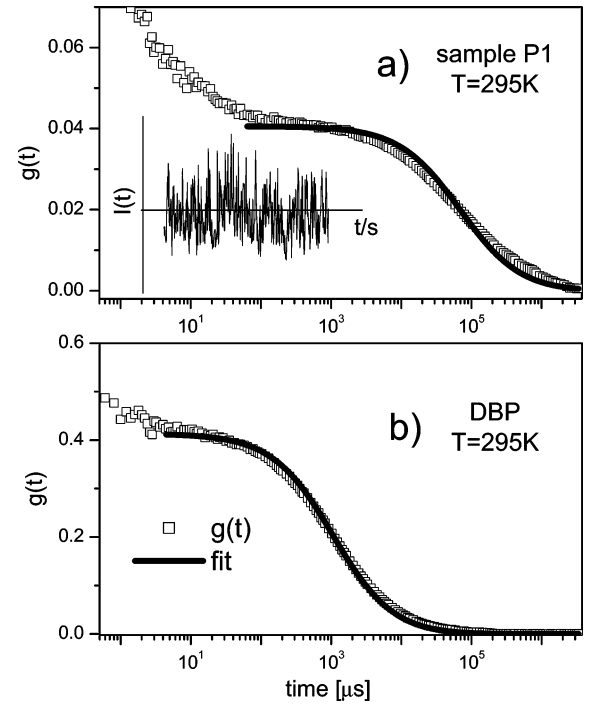

Figure 2. Fluorescence intensity correlation function $C(t)$ for Rh6G in (a) PBA (sample P1) and (b) DBP both at 295 K, along with their representations (solid lines) by eq 1. The featureless fluorescence intensity profile during the single recording time (90 s) is shown in the inset.

and DBP at 295 K and its representations by the following one-component model[1,2]

$$C(t) = g_t(t)\, g_d(t) \qquad (1)$$

where

$$g_t(t) = 1 + B \exp(-t/\tau_T) \qquad (2)$$

is the triplet decay with amplitude B and the characteristic time τ_T and

$$g_d(t) = N^{-1}[1 + (t/\tau_D)]^{-1}[1 + t/(f^2\tau_D)]^{-1/2} \qquad (3)$$

is the decay related to the 3D random diffusion of the pointlike particle during the time[2] $\tau_D = 0.25 r_0^2/D_s$, describing the average residence time of the particle in the focus area with lateral and longitudinal dimensions given by r_0 and z_0. N denotes the average number of particles in the focal volume, $f = z_0/r_0$, and D_s is the diffusion constant. The amplitude of $C(t)$ depends on the preceding instrumental factors and the number of Rh6G molecules in the analyzed system. Deviations from the nominal concentrations can be attributed to a nonuniform dye concentration. This, however, does not affect the conclusions concerning dynamics since the dye remains in the very dilute range. The focus dimension is computed from the value of τ_D (=30 ms) and the known diffusion coefficient of Rh6G in water (D = 2.8 × 10^{-6} cm^2/s), leading to r_0 = 160 nm.

The simple one-component model of particle diffusion does not represent very well the experimental correlation function. It should, however, be considered that we deal here with complex fluids in which a broadening of the relaxation with respect to such a model is not unexpected. Nevertheless, such a model can be taken as a reasonable approximation of the relaxation times for the well-defined experimental correlation functions. The corresponding diffusion time τ_D of Rh6G is found to assume very similar values (Table 1) in the three PBA films despite their vastly different macroscopic shear viscosities η ($\sim\tau_c$) but has a much lower value in DBP. Instead, τ_D appears to correlate with the local mobility of PBA as reflected in the segmental dynamics probed by DS and MS. This can be considered as an indication that the tracer Rh6G diffuses in the PBA matrix by rearrangements taking place together with displacements with the local macromolecular fragments moving with the characteristic segmental relaxation time τ_s. The three relaxation times in the PBA samples, as obtained from the present techniques, are shown in the Arrhenius plot of Figure 3. The very small but finite difference in the T_g's in the three PBA samples (values in Table 1 and dashed lines in Figure 3) of the extreme M_w's (P_1 and P_3 samples) is reflected in the τ_s (squares), whereas the expected M_w dependence is displayed by τ_c (open circles); the proximity of τ_D to τ_c in P1 is fortuitous. The two time scales τ_s and τ_D differ, however, by about 6 orders of magnitude.

The segmental relaxation of PBA probed by either DS or MS relates to local conformational rearrangements and segmental displacements with a characteristic nanoscopic length scale, b, known as dynamic cooperative length. Alternatively, the relatively long τ_D corresponds to the Rh6G diffusion over the much longer distance, d, in the illuminated volume, which can approach values up to $2z_0$. Hence, these two vastly apart time scales relate to a diffusional motion over different distances, i.e.

$$\tau_p/\tau_D \approx (b/d)^2 \qquad (4)$$

The length b is considered as a microscopic displacement relevant to the cooperative segmental rearrangements

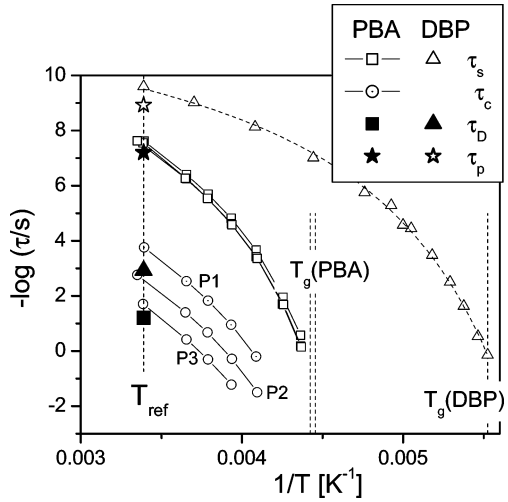

Figure 3. Activation plot of the different relaxation times for the three amorphous PBA and dibutyl phthalate (DBP) samples (Table 1). Open squares and circles denote the segmental τ_s and chain τ_c relaxation times of the three PBA samples. Open triangles denote the α-relaxation time τ_s of DBP represented by the WLF temperature equation (dashed line). The solid square and solid triangle are for the tracer diffusion of Rh6G in the three PBA matrices and in the glass former DBP, respectively. The open and solid stars denote the local relaxation time τ_p (eq 4) in DBP and PBA films. The vertical lines indicate the ambient temperature and the range of the glass transition temperatures T_g of the three PBA samples and DBP plasticizer.

of the matrix. The fluorescent dye can take part in such rearrangements with the microscopic relaxation time being of the order of τ_p. Molecular probes with sizes comparable to the polymer segments should take part in the segmental cooperative rearrangements and consequently reflect the segmental mobility which for long polymers is molecular weight independent. The observed insensitivity of τ_D to the molecular weight variations (and hence the viscosity) in the examined systems clearly implies that the dye diffusion reflects the local mobility of the polymer melts.

Assuming $b \approx 1$ nm of the order of the PBA segment size (the size of Rh6G is about 0.8 nm), τ_p is estimated to be at least 6 orders of magnitude shorter than τ_D. Hence, τ_p becomes well within an order of magnitude comparable with τ_s (see Table 1 and Figure 3). The remaining difference can be attributed to various effects, e.g., focus size estimation, size of the diffusant, and nonperfect coupling between the motions of the dye and of polymer segments. The FCS measurements are performed at $T \sim T_g + 70$ K far above T_g, and the observed relation between τ_D and τ_s due to coupling between probe and matrix motion is not unexpected. The reported breakdown of this relation due to enhanced translational diffusion occurs[5] at temperatures in the vicinity of T_g. Far above T_g, temperature does not significantly change τ_s (Figure 3). On the contrary, the variation of T_g is an effective way to change τ_s at high temperatures. In fact, the strong speed-up of the segmental motion in DBP relative to PBA at 295 K is fully reflected in the corresponding τ_D times of the FCS experiment. The tracer diffusion of radioactive penetrant molecules has been also used in earlier studies to estimate the monomeric friction of different polymer matrices.[12]

The assignment of the observed dynamics to the segmental motion associated with the primary α-relaxation opens new applications of FCS in polymer physics, enriching the battery of the experimental tools. Some examples of potential applications include matrix microrheology via tracking the mean-square displacement of large particles,[13] glass dynamics of thin films, inhomogeneous systems, diffusion in confined geometries,[14] and polymer brushes.

References and Notes

(1) Rigler, R.; Elson, E. L. *Fluorescence Correlation Spectroscopy*; Springer: Berlin, 2001.
(2) Lumma, D.; Keller, S.; Vilgis, T.; Rädler, J. O. *Phys. Rev. Lett.* **2003**, *90*, 218301.
(3) Mukhopadhyay, A.; Zhao, J.; Bae, S, C.; Granick, S. *Phys. Rev. Lett.* **2002**, *89*, 136103.
(4) Zettl, H.; Haefner, W.; Boeker, A.; Schmalz, H.; Lanzendoerfer, M.; Mueller, A.; Krausch, G. *Macromolecules* **2004**, *37*, 1917.
(5) Cicerone, M. T.; Blackburn, F. R.; Ediger, M. D. *Macromolecules* **1995**, *28*, 8224.
(6) Ehlich, D.; Sillescu, H. *Macromolecules* **1990**, *23*, 1600.
(7) Köhler, W.; Fytas, G.; Steffen, W.; Reinhardt, L. *J. Chem. Phys.* **1996**, *104*, 248.
(8) Michelman-Ribeiro, A.; Boukari, H.; Nossal, R.; Horkay, F. *Macromolecules* **2004**, *37*, 10212.
(9) Pakula, T.; Minkin, P.; Matyjaszewski, K. In *Advances in Controlled/Living Radical Polymerization*; Matyjaszewski, K., Ed.; *ACS Symp. Ser.* **2003**, *864*.
(10) Pakula, T. In *Broadband Dielectric Spectroscopy*; Kremer, F., Schönhals, A., Eds.; Springer: Berlin, 2003; Chapter 16.
(11) Williams, G.; McCrum, N. G.; Read, B. E. *Anelastic and Dielectric Effects in Polymeric Solids*; Dover Publ.: New York, 1991.
(12) Chen, S. P.; Ferry, J. D. *Macromolecules* **1968**, *1*, 270.
(13) Mason, T. G.; Weitz, D. A. *Phys. Rev. Lett.* **1995**, *74*, 1250.
(14) Sukhishvili, S. A.; Chen, Y.; Mueller, J. D.; Gratton, E.; Schweizer, K. S.; Granick, S. *Nature (London)* **2000**, *406*, 146.

MA047430K